

Reusable Cavitand-Based Electrospun Membranes for the Removal of Polycyclic Aromatic Hydrocarbons from Water

Mattia Amorini, Nicolò Riboni, Lucia Pesenti, Valentina Antonia Dini, Alessandro Pedrini, Chiara Massera, Chiara Gualandi, Federica Bianchi, Roberta Pinalli,* and Enrico Dalcanale*

In memory of François Diederich

The removal of toxic and carcinogenic polycyclic aromatic hydrocarbons (PAHs) from water is one of the most intractable environmental problems nowadays, because of their resistance to remediation. This work introduces a highly efficient, regenerable membrane for the removal of PAHs from water, featuring excellent filter performance and pH-driven release, thanks to the integration of a cavitand receptor in electrospun polyacrylonitrile (PAN) fibers. The role of the cavitand receptor is to act as molecular gripper for the uptake/release of PAHs. To this purpose, the deep cavity cavitand BenzoQxCav is designed and synthesized and its molecular structure is elucidated via X-Ray diffraction. The removal efficiency of the new adsorbent material toward the 16 priority PAHs is demonstrated via GC-MS analyses at ng L^{-1} concentration. A removal efficiency in the 32%, to 99% range is obtained. The regeneration of the membrane is performed by exploiting the pH-driven conformational switching of the cavitand between the vase form, where the PAHs uptake takes place, to the kite one, where the PAHs release occurs. The absorbance and regeneration capability of the membrane are successfully tested in four uptake/release cycles and the morphological stability.

organic compounds made of two or more aromatic rings, fused together in linear, angular, or cluster arrangements. They can be also referred as low-molecular weight PAHs (two or three rings) and high-molecular weight PAHs (four or more rings).^[3] These ubiquitous compounds can be generated from both anthropogenic activities, such as industrial, residential, and vehicular emissions, and natural phenomena, i.e., open burning, volcanic activities, and spills from coal deposits.^[2,3,5–7] The occurrence of PAHs has been assessed worldwide in different aquatic systems including influents and effluents from wastewater treatment plants, groundwater, surface- and sea-water.^[3] Currently, over 400 PAHs and derivatives have been identified and classified, but most regulations, analyses, and data are focused on only 14 to 20 PAH compounds.^[2,3,7]


PAHs are well-known toxic, mutagenic, either carcinogenic or suspected carcinogenic compounds, accumulating in human and animal tissues.^[2,3]

These compounds are characterized by high hydrophobicity and good lipid solubility due to their aromatic and delocalized structure: when their molecular weight increases, their aqueous solubility diminishes, whereas resistance to oxidation and reduction rises.^[2–4] PAHs absorption and bioaccumulation in several tissues, as well as their ubiquitous occurrence in the environment, pushed US EPA (United States Environmental Protection Agency) and EEA (European Environment Agency) to identify 24 PAH compounds as priority contaminants, thus introducing strict regulations for their monitoring.^[8–11] The 16 PAHs considered as priority pollutants by US EPA are: naphthalene, acenaphthylene, acenaphthene, fluorene, phenanthrene, anthracene, fluoranthene, pyrene, benz[a]anthracene, chrysene, benzo[b]fluoranthene, benzo[k]fluoranthene, benzo[a]pyrene, indeno[1,2,3-cd]pyrene, dibenz[a,h]anthracene, and benzo[ghi]perylene (Chart S1, Supporting Information). The European Union has set the maximum limit of $0.1 \mu\text{g L}^{-1}$ as sum of benzo[b]fluoranthene, benzo[k]fluoranthene, benzo[ghi]perylene, and indeno[1,2,3-cd]pyrene in water for human consumption, with a particular attention to benzo[a]pyrene limited to $0.01 \mu\text{g L}^{-1}$.^[12] The removal of PAHs represents one of the current challenges in environmental chemistry. Methods are based on biodegradation, chemical, and physical removal processes, often combined in order to obtain the highest degree of PAHs removal.^[2–4,6,7,13] Despite biological treatment methods have been proposed in municipal wastewater

1. Introduction

Water pollution and shortage of clean water are general global issues that are becoming urgent with the ongoing climate warming. Among the several pollutants present in water, polycyclic aromatic hydrocarbons (PAHs) have received particular attention in the last years, because of their carcinogenicity and persistency in the environment.^[1–4] PAHs are a class of hazardous

M. Amorini, N. Riboni, A. Pedrini, C. Massera, F. Bianchi, R. Pinalli, E. Dalcanale
Dipartimento di Scienze Chimiche, della Vita e della Sostenibilità Ambientale and INSTM Udr Parma
Università di Parma
Parco Area delle Scienze 17/A, Parma 43123, Italy
E-mail: roberta.pinalli@unipr.it; enrico.dalcanale@unipr.it
L. Pesenti, V. A. Dini, C. Gualandi
Dipartimento di Chimica “G. Ciamician” and INSTM Udr Bologna
Università di Bologna
Via Selmi 2, Bologna 40126, Italy

 The ORCID identification number(s) for the author(s) of this article can be found under <https://doi.org/10.1002/smll.202104946>.

© 2021 The Authors. Small published by Wiley-VCH GmbH. This is an open access article under the terms of the Creative Commons Attribution License, which permits use, distribution and reproduction in any medium, provided the original work is properly cited.

DOI: 10.1002/smll.202104946

treatment plants,^[2,3,13] the most commonly applied methods are based on physicochemical processes, including photodegradation, oxidation, coagulation, and sorption.^[2-4,6,7] However, current treatments involving advanced oxidation and ozonation processes are affected by the formation of partial oxidized by-products which, in several cases, are more toxic than the parent molecules.^[14]

Adsorption is the simplest, fastest, and broadly applicable remediation technology: in the past 15 years, several materials have been proposed for PAHs removal from water, including activated carbon, nanotubes, biochar, engineered clays, and amberlite XAD-2.^[3,6,7,15,16] The main disadvantage in the use of particle sorbents relies in the difficult removal of the material from the remediated water. Another approach gaining increasing attention is the use of polymeric membranes due to the high energy efficiency, low-cost, ease of preparation, mechanical properties, and easy separation from the remediated solution.^[6,7,17-20] Recently, electrospinning has been proposed as an efficient and convenient technique for the production of nanofibrous membranes for the removal of several aquatic pollutants, including PAHs. The main advantages of electrospun materials rely on good mechanical properties, high surface area-to-volume ratios, and possibility to tune the membrane porosity, combined with the ease of the approach and scalability.^[21,22] Functionalization with activated carbon^[23] and laccase^[24,25] has been proposed either to improve fiber adsorption capabilities or to promote PAHs degradation. Another interesting approach is the use of membranes embedded with molecular receptors to increase membrane selectivity. There are only a handful of reports on this topic, using cyclodextrins.^[26-29] Cyclophanes and metallacycles have proved to be selective receptors for the uptake of some PAHs in water,^[30-32] but their recognition prowess has not been exploited into polymeric membranes so far.

Calixarenes and cavitands are synthetic macrocycles presenting enforced cavities of molecular dimensions, which have been used as adsorbent materials for organic pollutants in water.^[33-37] In particular, polymer adsorbents based on quinoxaline cavitands are effective in the uptake of chlorinated aromatic^[38] and aliphatic^[39] hydrocarbons. Their complexation properties in water are defined by the combination of two major factors: the hydrophobicity of the guest, which determines its affinity for the hydrophobic cavity, and shape complementarity.^[35]

Here, we introduce a new, regenerable functionalized membrane for the removal of PAHs from water, featuring high filter performance and pH-driven release, thanks to the integration of an ad hoc synthesized deep cavity cavitand in electrospun polyacrylonitrile (PAN) fibers.

2. Results and Discussion

Quinoxaline-based cavitands have shown to be suitable receptors for the selective uptake of aromatic and chlorinated compounds from water^[34-36,40] and air,^[41] leading to their use as adsorbent materials in sensors for BTEX monitoring.^[42-44] However, quinoxaline cavitands (QxCav, **Figure 1a**) are not suitable for PAHs uptake, since PAHs are too large to fit into their 5.8 Å deep cavity. Cavitands equipped with deeper hydrophobic cavities, suitable to host bulky guest molecules, are required to reach the goal.

Based on these premises, we designed and synthesized the new deep cavity cavitand BenzoQxCav (**Figure 1a**), extending

the length of the aromatic walls through the functionalization of the resorcinarene scaffold with four benzoquinoxaline walls at the upper rim. The resulting BenzoQxCav features a 2.5 Å deeper hydrophobic cavity compared to the parent QxCav, to promote PAHs inclusion.

2.1. BenzoQxCav Synthesis

The receptor was prepared following a convergent synthetic approach (Scheme S1, Supporting Information), which comprises: i) synthesis of the benzoquinoxaline bridging unit **1**, and ii) synthesis of the target cavitand BenzoQxCav. The 2,3-dichlorobenzoquinoxaline wall **1** was synthesized in two steps starting from 2,3-diaminonaphthalene, accordingly to a modified literature procedure.^[45] Hexyl-footed resorcinarene was reacted with the bridging unit **1** in presence of potassium carbonate as base and DMF as solvent. BenzoQxCav was obtained as a bright yellow solid in 86% yield after recrystallization from ethyl acetate and characterized by NMR spectroscopy (Figures S1 and S2, Supporting Information) and MALDI-TOF spectrometry (Figure S3, Supporting Information).

2.2. Crystal Structure Determination

The structure of the new cavitand was investigated through X-ray diffraction analysis and computational studies. Suitable

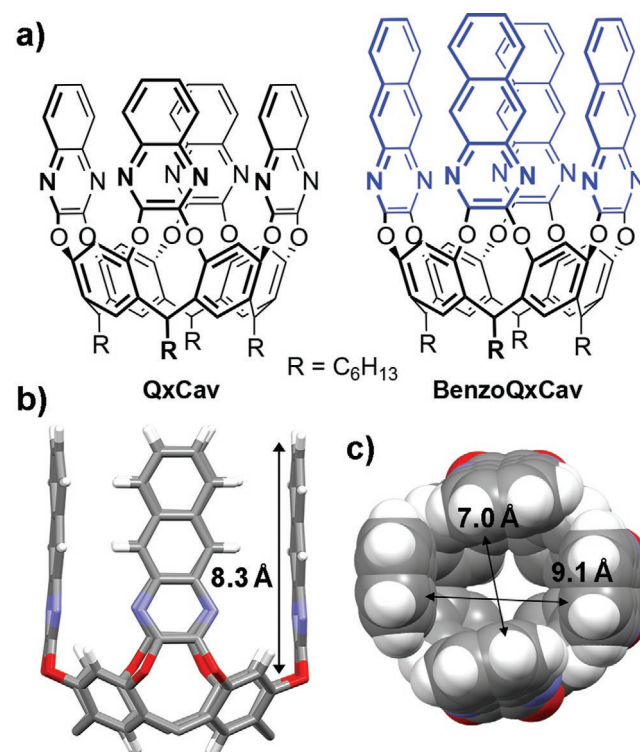


Figure 1. a) Chemical structure of QxCav versus BenzoQxCav; b) side view of the molecular structure of BenzoQxCav (capped stick style); and c) top view of BenzoQxCav (space fill style) with cavity opening dimensions. The lower rim alkyl substituents of the receptor are pruned for clearness. Color code: carbon: gray; nitrogen: blue; oxygen: red; hydrogen: white.

single crystals were obtained by slow evaporation of a solution of BenzoQxCav in DMF (Figure S4, Supporting Information).

The molecular structure shows that the cavita nd adopts the closed vase conformation in the solid state. Two DMF molecules are present in the crystal structure: one among the alkyl chains and one disordered over two positions with equal occupancy, either perched on top of the cavity or enfolded by it. The introduction of an additional fused ring at the upper rim provides a deeper cavity (≈ 8.3 Å deep, Figure 1b) compared to the parent QxCav (≈ 5.8 Å deep). These values refer to the distance between the mean plane passing through the eight oxygen atoms of the resorcinol-based cavity and the eight external carbon atoms of the upper aromatic rings. The choice of the plane crossing the oxygens as floor of the cavity is dictated by the evidence that, in all crystal structures of host–guest complexes between QxCav and aromatic guests, the guest never gets deeper.^[41] The introduction of the benzoquinoxaline walls provides a cavita nd with an upper rim opening of ≈ 9.1 Å \times 7.0 Å (Figure 1c, the shortest distances between carbon atoms of the upper aromatic rings belonging to opposite walls have been reported). The dimensions of the cavity entrance partially limit the PAHs uptake, although the cavity walls are breathing even in the solid state, so they can adjust their distance to some extent according to the size of the guest.^[46]

The crystallographic data were used as starting point to analyze the dimension of the cavity through theoretical methods. The molecule surface was evaluated with Yasara computational software, which allows to estimate the cavity size (Figure S5, Supporting Information).^[47] The accessible free volume inside the cavity was calculated using Caver software and Depth web server, obtaining an internal volume of 247 Å³ against the 166 Å³ of the parent QxCav (Figure S6, Supporting Information).^[48,49]

2.3. Solid-Phase Microextraction-Gas Chromatography-Mass Spectrometry (SPME-GC-MS) Analysis

SPME-GC-MS analyses were preliminarily performed in order to evaluate the extraction capabilities of the developed BenzoQxCav toward the target PAHs in water samples. Commercial silica fibers properly coated with the powdered BenzoQxCav were used for the extraction of the 16 PAHs. The thermal stability of the BenzoQxCav was assessed by means of thermogravimetric analysis (TGA), resulting in a weight loss lower than 10% up to 400 °C (Figure S7, Supporting Information). The thermal stability was further confirmed by the absence of bleeding when the fibers were desorbed at 270 °C in the GC injection port.

Finally, the performance of the BenzoQxCav-coated silica fibers was investigated in terms of enrichment factors (EFs),^[50] by analyzing tap-water samples spiked with 100 ng L⁻¹ of each analyte (Figure 2), obtaining EFs in the 11 760(\pm 970)–119 000(\pm 12 000) range. The obtained results demonstrate the high affinity of the developed coating for all the investigated analytes. As expected, the lowest EF values were achieved for the heaviest PAHs, namely indeno(1,2,3-cd)pyrene, dibenzo[a,h]anthracene, and benzo(ghi)perylene: this behavior can be rationalized considering that the bulkiness of these compounds limits their uptake by the hydrophobic cavity.

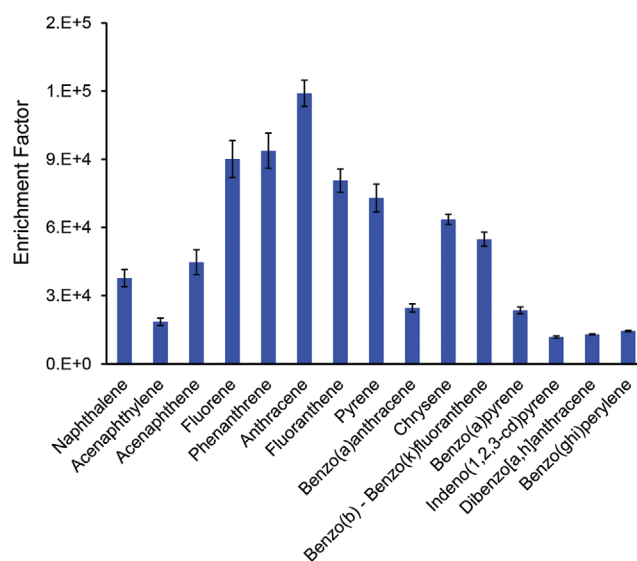


Figure 2. Enrichment factors (EFs) of the BenzoQxCav silica fiber. Extraction time: 45 min, extraction temperature: 60 °C, desorption temperature: 270 °C, desorption time: 2 min ($n = 3$). Benzo(b) and benzo(k)fluoranthene are detected together.

2.4. Electrospun Fibers Preparation and Characterization

The efficient filtration of micropollutants from water requires the integration of BenzoQxCav into a polymeric membrane. Electrospinning was selected as the technology of choice to produce flexible membranes with high surface area and interconnected microporosity,^[51,52] and to guarantee efficient adsorption and high flow rate. This technology is notably advantageous in this framework, since fibers can be doped with functional molecules by simply dissolving the cavita nd in the starting electrospun solution. This straightforward one-step approach for the preparation of ready-to-use fibers is prospectively more easily scalable when compared to multistep routes, such as surface covalent grafting or physical absorption.^[53,54]

Several polymeric matrices have been used for the incorporation of cyclodextrins into electrospun fibers, including polystyrene,^[55] polymethylmethacrylate,^[56] and cellulose.^[26] In our case, PAN was chosen as fiber matrix for the BenzoQxCav embodiment, since PAN is a common material used in potable reuse membranes; it has an acceptable mechanical strength, improved by electrospinning process, good hydrophilicity,^[57] and it is stable under both basic and acid conditions.^[58,59] Moreover, PAN does not form inclusion complexes with quinoxaline cavita nds .

A new filtrating material was prepared by electrospinning PAN dissolved in DMF after the addition of a proper amount of cavita nd to achieve a final concentration of 6 wt% BenzoQxCav in the fibers. Being the cavita nd completely soluble in DMF under the applied concentration, the obtained solution was homogeneous, consequently no loss of cavita nd was evidenced during the process. The resulting membrane was made up by thin continuous defect-free fibers with average diameter 0.25 (\pm 0.06) μm (Figure 3). The addition of BenzoQxCav to the starting solution slightly, albeit significantly, increased the fiber diameters ($p < 0.0001$) as well as the fiber hydrophobicity. This

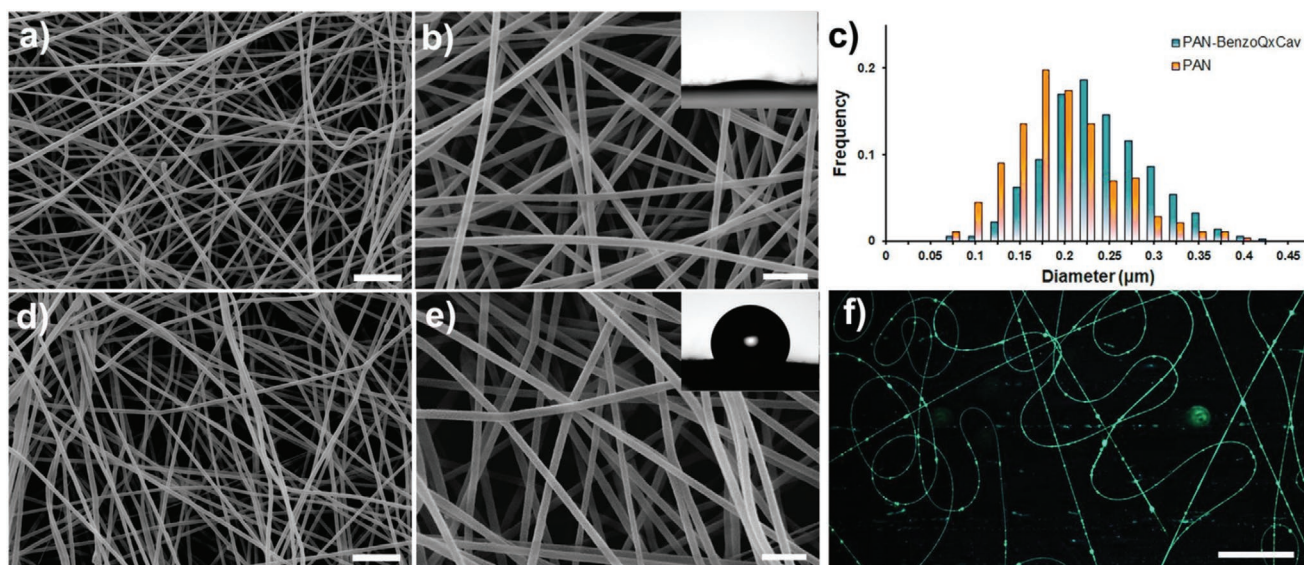


Figure 3. a,b) SEM images of polyacrylonitrile (PAN) fibers; d,e) SEM images of PAN-BenzoQxCav fibers; c) fiber diameter distributions; f) confocal scanning fluorescence images of PAN-BenzoQxCav. Scale bars: a, d = 5 μm ; b, e = 2 μm ; f = 100 μm . Insets: shape of a water drop on b) PAN and e) PAN-BenzoQxCav fibers (WCA = $117 \pm 5^\circ$).

is evident from the water contact angle behavior: water almost instantaneously penetrates the pores of sole PAN membrane (inset Figure 3b) while it is not absorbed by PAN-BenzoQxCav mat (inset Figure 3e). This finding, together with the strong fluorescent emission of cavitant loaded fibers (Figure 3f) and ATR-IR spectra (Figure S8, Supporting Information), confirms the presence of BenzoQxCav at the fiber surface. The macroscopic appearance of the electrospun PAN and PAN-BenzoQxCav mats detached from the metallic collector are shown in Figure S9 (Supporting Information).

2.5. Membrane Performance in PAHs Removal

The filtration experiments were carried out by using water samples containing 16 PAHs, each at 100 ng L^{-1} . This concentration level was selected taking into account the possible use of the membrane for drinking water purification. Both unfunctionalized and functionalized membranes were used in a frit-type filter and tested for PAHs removal (Figure S10, Supporting Information). The removal capability of the developed material was assessed by calculating the amount of analytes present in the filtered solution with respect to the concentration levels spiked into the water sample prior to membrane filtering.

As shown in Figure 4, the functionalized material (green bars) was characterized either by better or not significantly different performance compared to unfunctionalized PAN mats (yellow bars), depending on the PAHs nature. More precisely, the low-molecular weight and less hydrophobic PAHs (128–202 Da) were weakly adsorbed by the unfunctionalized PAN, whereas higher adsorption was observed for the heaviest PAHs, for which removal percentages in the 82.2(± 3.6)–96.4(± 0.4)% range were obtained. PAN membranes containing BenzoQxCav (green bars) were characterized by

enhanced removal capabilities toward low-molecular weight and less bulky PAHs (from naphthalene to chrysene), with the exception of acenaphthylene. It is interesting to note that the heaviest PAHs were also retained in a very efficient way, up to $99.1 \pm 0.4\%$. The slight difference in terms of high-molecular weight PAHs removal between the functionalized and unfunctionalized materials suggests the existence of physisorption processes mainly via hydrophobic interactions with PAN polymer chains that favor the adsorption of the heaviest pollutants onto the membranes. Therefore, not all the PAHs removal can be attributed exclusively to cavity inclusion. For these PAHs, the sum of the specific and unspecific sorption process leads to their almost complete removal after a single filtration step.

The size of the 16 PAH micropollutants was estimated by density functional theory (DFT) calculations and modeled using Mercury 2020. The data are reported in Table S2 (Supporting Information). The seven most retained PAHs by the PAN-BenzoQxCav mat have dimensions compatible with the almost complete engulfment into the cavity (length < 10 \AA and width < 7 \AA), supporting the experimental adsorption data.

The adsorption kinetics of the pristine PAN and PAN-BenzoQxCav membranes were evaluated to assess the influence of the cavitant on the overall adsorption, by analyzing water samples spiked with 50 $\mu\text{g L}^{-1}$ of each PAH (800 $\mu\text{g L}^{-1}$ overall). During the first 30 min, a fast adsorption stage occurred, followed by a second step during which the adsorption rate was slowed down (Figure S11, Supporting Information). These findings suggest that during the first step a greater number of adsorption sites are available, thus allowing the fast removal of the analytes; then, when the availability of these sites is reduced, the adsorption rate is slowed down. The functionalized membrane is characterized by higher sorption capacities compared to those of bare PAN (Figure S11, Supporting Information).

The adsorption kinetics of the functionalized membrane was investigated by calculating the correlation coefficients of

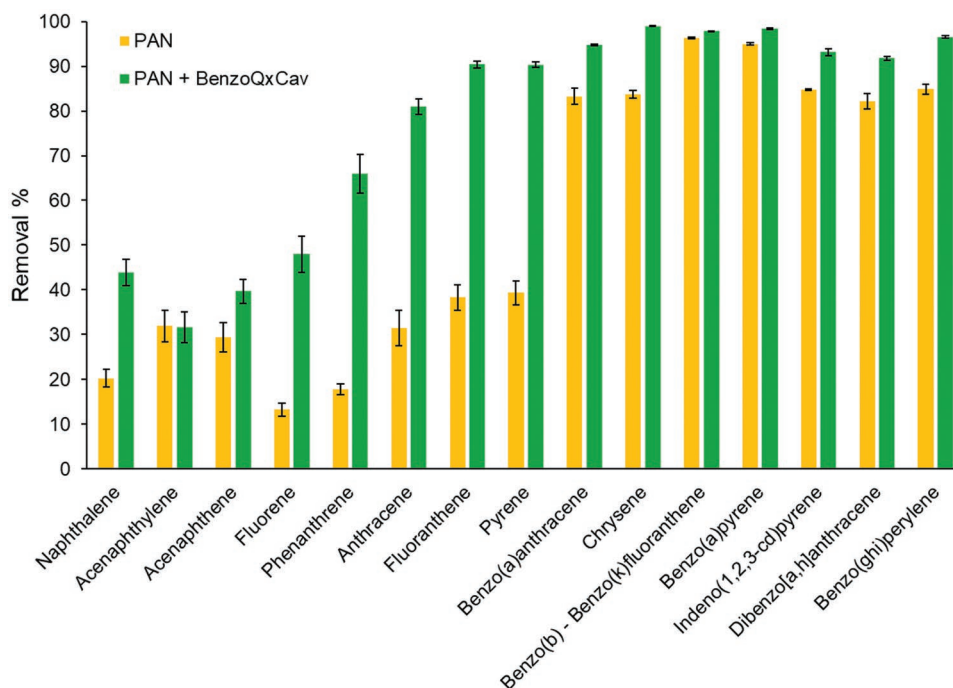


Figure 4. Desorption profile of pristine polyacrylonitrile (PAN) electrospun (yellow bars) and PAN-BenzoQxCav (green bars).

both the pseudo-first order and pseudo-second order models, being the R^2 value of pseudo-second-order model ($R^2 = 0.9996$) superior to that achieved by the pseudo-first-order one ($R^2 = 0.9632$) (Figure S12, Supporting Information). By using the pseudo-second-order model, a very good agreement between the calculated and the experimental q_e value was obtained (Table S3, Supporting Information), as already reported in previous studies.^[22,28]

2.6. Regeneration and Reuse of the Electrospun Membranes

A critical issue in water purification is the regeneration of the contaminated membranes. In the case of activated carbon, the workhorse of water purification, thermal regeneration is commonly applied due to its simplicity and versatility.^[60] However, restoring the initial performances can be difficult, time-consuming, and expensive. In this context, reusable membranes featuring a molecularly controlled uptake and release of the trapped contaminants are appealing alternatives. Despite of the attractiveness of the approach, there is just a couple of studies reporting the salt^[61] or light-driven^[62] release of organic pollutants from a porous material. To address this issue, we leveraged the unique ability of quinoxaline cavitands to switch between two equivalent conformations, namely the close vase and the open kite.^[63] The PAH cavity inclusion takes place in the vase form, while the release requires the switch to the kite form (Figure 5a).

The conformational equilibrium between vase and kite forms is influenced by several factors^[64] operating also in polymeric matrices,^[65,66] among which the pH is the easiest to implement in the present case.^[67] The mildly basic behavior of the N-atoms of benzoquinoxaline walls (the pKa of the protonated

quinoxaline nitrogen is 1.67),^[68] makes possible their protonation by a strong acid, such as trifluoroacetic acid (TFA). The protonated form of the quinoxaline walls leads to a mutual electrostatic repulsion and the consequent opening of the cavitand from the vase to the kite form.

The deepening of the cavity does not affect the unique vase-kite conformational equilibrium, as demonstrated by UV and fluorescence experiments in solution on BenzoQxCav (see Figures S13–S18, Supporting Information, for the detailed analyses and control experiments in solution).

The pH-driven conformational switch was then investigated in the PAN membrane integrated with BenzoQxCav, to verify its effectiveness in the solid material. The filtration of a TFA aqueous solution through the electrospun material provided a partial quench of the fluorescence emission in the solid state (Figure 5c), as observed in the solution tests (Figure 5b), as indication of the progressive vase-to-kite conformational switch of the BenzoQxCav. The saturation was achieved after the filtration of 20 mL of TFA solution, leading to a 50% reduction of the total fluorescence emission of the pristine material. The subsequent filtration of an ammonia aqueous solution over the quenched electrospun material allowed the complete restore of its fluorescence emission, leading to the reverse switch to the vase conformer. The incomplete switching in the solid state is justified by the partial solvent accessibility of BenzoQxCav in the PAN matrix. Part of it is deeply buried into the PAN matrix, rendering it inaccessible to the acid/base water solutions.

The pH-driven vase-to-kite switch in the solid state was then exploited to regenerate the PAN-BenzoQxCav fibers. After the first extraction cycle was completed (Figure 5d), the PAN-BenzoQxCav mats maintained unaltered their original fibrous morphology (Figure S19a, Supporting Information), and were regenerated using 30 mL of a TFA aqueous solution (pH = 1.5)

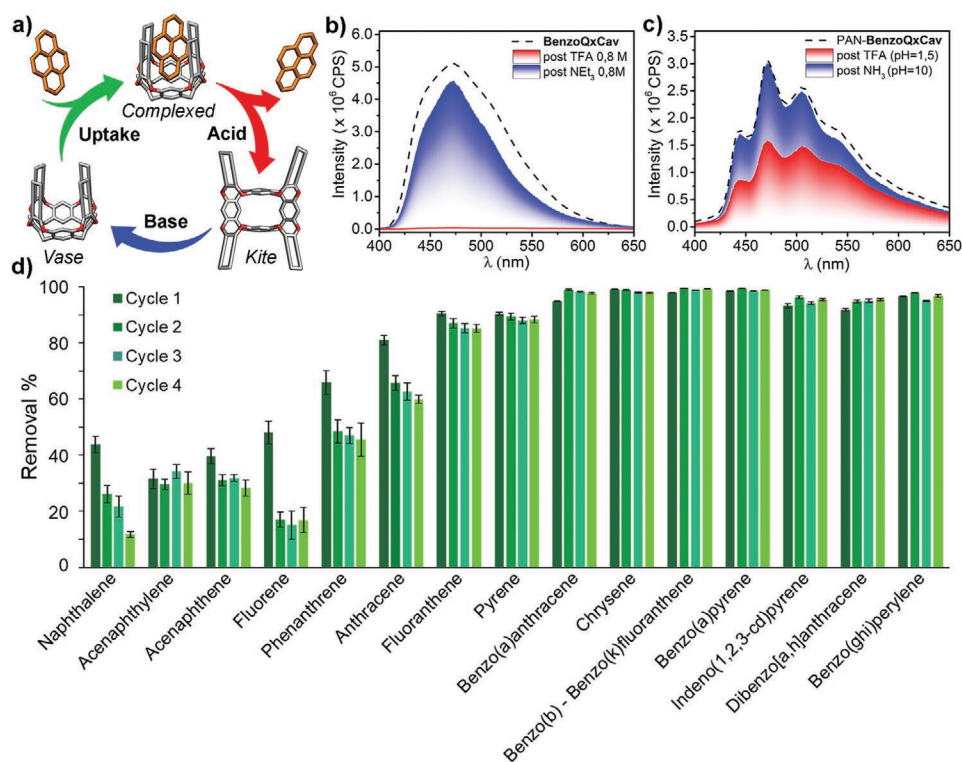


Figure 5. a) Schematic representation of pH-driven PAHs uptake and release by BenzoQxCav; b) changes of the fluorescence emission of BenzoQxCav (1.9×10^{-5} M) in DCM solution upon addition of TFA and NEt_3 ; c) changes of the fluorescence emission of PAN-BenzoQxCav after filtration with trifluoroacetic acid (TFA) and NH_3 aqueous solutions; d) removal capability of PAN-BenzoQxCav membranes after four regeneration steps.

to induce the opening to the kite form and the release of complexed PAHs. This was followed by filtration with 20 mL of distilled water until neutral pH. Then a basic treatment was performed to restore the BenzoQxCav vase form. The PAN-BenzoQxCav composite was treated with 20 mL of an ammonia aqueous solution (pH = 10) to deprotonate the nitrogen atoms of the benzoquinoline walls. An additional washing step with 20 mL of distilled water was performed to return the PAN-BenzoQxCav mats to neutral pH (for details see the regeneration procedure in the Supporting Information). SEM analysis assessed that membrane morphology was unaffected by both acid and basic treatments (Figure S19b,c, Supporting Information). After the first regeneration protocol was completed, the membrane was reused for new cycles of PAHs removal. More precisely, the regeneration capability of the membranes was tested by performing four filtration cycles each followed by the already described regeneration steps (Figure 5d). A good reusability of the BenzoQxCav membranes was observed: the analysis of variance did not show the presence of significant differences ($p > 0.05$) in the removal of 12 out of 16 PAHs, whereas a remarkable decrease in the adsorption capability of the mats was observed in the case of naphthalene and fluorene, after the first regeneration step. The morphological stability of the membrane was also assessed by SEM analysis (Figure S19d, Supporting Information). As expected, no significant differences in terms of removal capability were observed when the unfunctionalized PAN membrane was used (Figure S20, Supporting Information).

We also tested the leakage of the membrane under acidic, neutral, and basic water conditions to verify any release of BenzoQxCav in water. The filtered water in all three cases was analyzed by fluorescence spectroscopy since BenzoQxCav is highly fluorescent and it can be detected even at very low concentration. No fluorescence was detected in the filtered aqueous medium, thus ruling out any leakage of the cavitant under the membrane working conditions.

3. Conclusions

A reusable membrane for the removal of PAHs from contaminated water has been produced by embedding a cavitant receptor in an electrospun PAN matrix, with a straightforward and scalable one step production process. The crafted cavitant presents a 8.3 Å deep hydrophobic cavity capable to engulf the PAH pollutants with high efficiency at the solid–water interface, and works as molecular gripper^[69] to allow their reversible encapsulation/release via a pH-driven conformational switch. Exposure of the PAN-BenzoQxCav electrospun membrane to water contaminated with trace amounts of 16 PAHs resulted in a significant boost in the removal of the eight lighter contaminants compared to the pristine PAN membrane, driven by cavity inclusion. The regeneration of the PAN-BenzoQxCav membrane relies on the release of the bound PAHs upon conformational switch from the closed vase to the open kite form, triggered by exposure of the membrane to a water solution of

TFA, followed by aqueous ammonia treatment to restore the vase conformer. Repeated regeneration cycles do not significantly alter the morphology and activity of the membrane.

Overall, the unique absorbance and regeneration properties of the PAN-BenzoQx Cav membrane are the result of the incorporation of a switchable cavitand receptor featuring a large hydrophobic cavity into a robust, high surface area electrospun PAN membrane.

4. Experimental Section

A detailed description of cavitand synthesis, mats fabrication process, computational studies, crystallographic analyses, GC-MS analyses, and characterizations can be found in the Supporting Information.

Supporting Information

Supporting Information is available from the Wiley Online Library or from the author.

Acknowledgements

Dr. Damiano Genovese is warmly acknowledged for confocal microscopy analyses. This work was benefited from the equipment and framework of the COMP-HUB Initiative, funded by the “Departments of Excellence” program of the Italian Ministry for Education, University and Research (MIUR, 2018–2022). The authors acknowledge MIUR through the PRIN project 20179BJNA2 for financial support. The authors acknowledge the Centro Interdipartimentale di Misure “G. Casnati” of the University of Parma for the use of NMR and MS facilities.

Open access funding provided by Università degli Studi di Parma within the CRUI-CARE Agreement.

Conflict of Interest

The authors declare no conflict of interest.

Data Availability Statement

The data that supports the findings of this study are available in the supplementary material of this article.

Keywords

cavitands, electrospinning, PAHs, reusable membranes, water treatment

Received: August 17, 2021

Revised: October 13, 2021

Published online: November 9, 2021

- [1] A. T. Lawal, *Cogent Environ. Sci.* **2017**, 3, 1339841.
 [2] H. I. Abdel-Shafy, M. S. M. Mansour, *Egypt. J. Pet.* **2016**, 25, 107.
 [3] A. Mojiri, J. L. Zhou, A. Ohashi, N. Ozaki, T. Kindaichi, *Sci. Total Environ.* **2019**, 696, 133971.
 [4] G. K. Gaurav, T. Mehmood, M. Kumar, L. Cheng, K. Sathishkumar, A. Kumar, D. Yadav, *J. Contam. Hydrol.* **2021**, 236, 103715.
 [5] M. Qiao, Y. Bai, W. Cao, Y. Huo, X. Zhao, D. Liu, Z. Li, *Chemosphere* **2018**, 211, 185.

- [6] M. Smol, M. Włodarczyk-Makuła, *Polycyclic Aromat. Compd.* **2017**, 37, 292.
 [7] S. Lamichhane, K. C. Bal Krishna, R. Sarukkalige, *Chemosphere* **2016**, 148, 336.
 [8] L. H. Keith, *Polycyclic Aromat. Compd.* **2015**, 35, 147.
 [9] C. Lestingi, T. Tavoloni, V. Bardeggia, M. Perugini, A. Piersanti, *Food Addit. Contam., Part A: Chem., Anal., Control, Exposure Risk Assess.* **2017**, 34, 1140.
 [10] D. Lerda, *JRC Tech. Notes* **2010**, 3, 1.
 [11] N. Metal, C. Wastes, N. Metal, C. Wastes, *National Primary Drinking Water Regulations, Federal Register; 40 CFR Chapter I, Part 141*, US EPA, Washington, DC **1991**.
 [12] Council of the European Union, Council Directive 98/83/EC of 3 November 1998 on the quality of water intended for human consumption (O) L 330 05.12.1998 p. 32). *Documents in European Community Environmental Law* **1998**.
 [13] B. K. Behera, A. Das, D. J. Sarkar, P. Weerathunge, P. K. Parida, B. K. Das, P. Thavamani, R. Ramanathan, V. Bansal, *Environ. Pollut.* **2018**, 241, 212.
 [14] O. M. Rodriguez-Narvaez, J. M. Peralta-Hernandez, A. Goonetilleke, E. R. Bandala, *Chem. Eng. J.* **2017**, 323, 361.
 [15] L. M. Frescura, H. A. Pereira, F. V. da Silva, B. B. de Menezes, M. Hilgemman, A. P. Lazzaretti, P. C. do Nascimento, M. B. da Rosa, *Polycyclic Aromat. Compd.* **2020**, 40, 1347.
 [16] A. A. Akinpelu, M. E. Ali, M. R. Johan, R. Saidur, M. A. Qurban, T. A. Saleh, *Process Saf. Environ. Prot.* **2019**, 122, 68.
 [17] S. Li, J. Luo, X. Hang, S. Zhao, Y. Wan, *J. Membr. Sci.* **2019**, 582, 264.
 [18] J. A. S. Costa, V. H. V. Sarmiento, L. P. C. Romão, C. M. Paranhos, *J. Membr. Sci.* **2020**, 601, 117912.
 [19] J. A. S. Costa, V. H. V. Sarmiento, L. P. C. Romão, C. M. Paranhos, *Silicon* **2021**, <https://doi.org/10.1007/s12633-021-01165-6>.
 [20] C. Gong, H. Huang, Y. Qian, Z. Zhang, H. Wu, *RSC Adv.* **2017**, 7, 52366.
 [21] A. Senthamizhan, B. Balusamy, T. Uyar, in *Filtering Media by Electrospinning: Next Generation Membrane for Separation Applications*, (Eds: M. L. Focarete, C. Gualandi, S. Ramakrishna), Springer, Berlin **2018**; pp. 115–150.
 [22] Y. Dai, J. Niu, L. Yin, J. Xu, Y. Xi, *J. Hazard. Mater.* **2011**, 192, 1409.
 [23] M. J. Soberman, R. R. Farnood, S. Tabe, *Sep. Purif. Technol.* **2020**, 253, 117461.
 [24] Y. Dai, L. Yin, J. Niu, *Environ. Sci. Technol.* **2011**, 45, 10611.
 [25] Y. Dai, J. Niu, L. Yin, J. Xu, J. Xu, *Sep. Purif. Technol.* **2013**, 104, 1.
 [26] A. Celebioglu, S. Demirci, T. Uyar, *Appl. Surf. Sci.* **2014**, 305, 581.
 [27] F. Topuz, T. Uyar, *J. Hazard. Mater.* **2017**, 335, 108.
 [28] A. Celebioglu, F. Topuz, Z. I. Yildiz, T. Uyar, *ACS Omega* **2019**, 4, 7850.
 [29] J. M. Racicot, T. L. Mako, A. Healey, B. Hos, M. Levine, *ChemPlusChem* **2020**, 85, 1730.
 [30] E. J. Dale, N. A. Vermeulen, A. A. Thomas, J. C. Barnes, M. Juríček, A. K. Blackburn, N. L. Strutt, A. A. Sarjeant, C. L. Stern, S. E. Denmark, J. F. Stoddart, *J. Am. Chem. Soc.* **2014**, 136, 10669.
 [31] M. D. García, C. Alvarino, E. M. López-Vidal, T. Rama, C. Peinador, J. M. Quintela, *Inorg. Chim. Acta* **2014**, 417, 27.
 [32] V. Martínez-Agramunt, S. Ruiz-Botella, E. Peris, *Chem. - Eur. J.* **2017**, 23, 6675.
 [33] T. Skorjanc, D. Shetty, A. Trabolsi, *Chem* **2021**, 7, 882.
 [34] E. Dalcanale, G. Costantini, P. Soncini, *J. Inclusion Phenom. Mol. Recognit. Chem.* **1992**, 13, 87.
 [35] E. Dalcanale, J. Hartmann, *Sens. Actuators, B* **1995**, 24, 39.
 [36] J. Hartmann, P. Hauptmann, S. Levi, E. Dalcanale, *Sens. Actuators, B* **1996**, 35, 154.
 [37] A. Giri, M. D. W. Hussain, B. Sk, A. Patra, *Chem. Mater.* **2019**, 31, 8440.
 [38] M. Giannetto, A. Pedrini, S. Fortunati, D. Brando, S. Milano, C. Massera, R. Tatti, R. Verucchi, M. Careri, E. Dalcanale, R. Pinalli, *Sens. Actuators, B* **2018**, 276, 340.

- [39] L. P. Skala, A. Yang, M. J. Klemes, L. Xiao, W. R. Dichtel, *J. Am. Chem. Soc.* **2019**, *141*, 13315.
- [40] F. Bianchi, M. Mattarozzi, P. Betti, F. Bisceglie, M. Careri, A. Mangia, L. Sidisky, S. Ongarato, E. Dalcanale, *Anal. Chem.* **2008**, *80*, 6423.
- [41] R. Pinalli, A. Pedrini, E. Dalcanale, *Chem. Eur. J.* **2018**, *24*, 1010.
- [42] S. Zampolli, P. Betti, I. Elmi, E. Dalcanale, *Chem. Commun.* **2007**, *0*, 2790.
- [43] P. Clément, S. Korom, C. Struzzi, E. J. Parra, C. Bittencourt, P. Ballester, E. Llobet, *Adv. Funct. Mater.* **2015**, *25*, 4011.
- [44] J. W. Trzciński, R. Pinalli, N. Riboni, A. Pedrini, F. Bianchi, S. Zampolli, I. Elmi, C. Massera, F. Ugozzoli, E. Dalcanale, *ACS Sens.* **2017**, *2*, 590.
- [45] O. B. Berryman, A. C. Sather, J. Rebek, *Org. Lett.* **2011**, *13*, 5232.
- [46] L. D. Shirtcliff, H. Xu, F. Diederich, *Eur. J. Org. Chem.* **2010**, *2010*, 846.
- [47] E. Krieger, G. Koraimann, G. Vriend, *Proteins: Struct., Funct., Genet.* **2002**, *47*, 393.
- [48] K. P. Tan, R. Varadarajan, M. S. Madhusudhan, *Nucleic Acids Res.* **2011**, *39*, W242.
- [49] E. Chovancova, A. Pavelka, P. Benes, O. Strnad, J. Brezovsky, B. Kozlikova, A. Gora, V. Sustr, M. Klvana, P. Medek, L. Biedermannova, J. Sochor, J. Damborsky, *PLoS Comput. Biol.* **2012**, *8*, e1002708.
- [50] N. Riboni, J. W. Trzcinski, F. Bianchi, C. Massera, R. Pinalli, L. Sidisky, E. Dalcanale, M. Careri, *Anal. Chim. Acta* **2016**, *905*, 79.
- [51] Y. Jia, G. Scitutto, R. Mazzeo, C. Samorì, M. L. Focarete, S. Prati, C. Gualandi, *ACS Appl. Mater. Interfaces* **2020**, *12*, 39620.
- [52] G. Pagnotta, G. Graziani, N. Baldini, A. Maso, M. L. Focarete, M. Berni, F. Biscarini, M. Bianchi, C. Gualandi, *Mater. Sci. Eng., C* **2020**, *113*, 110998.
- [53] R. Gentsch, F. Pippig, S. Schmidt, P. Cernoch, J. Polleux, H. G. Börner, *Macromolecules* **2011**, *44*, 453.
- [54] U. Montanari, D. Cocchi, T. M. Brugo, A. Pollicino, V. Taresco, M. R. Fernandez, J. C. Moore, D. Sagnelli, F. Paradisi, A. Zucchelli, S. M. Howdle, C. Gualandi, *Polymers* **2021**, *13*, 1804.
- [55] T. Uyar, R. Havelund, J. Hacaloglu, K. F. Besenbacher, P. Kingshott, *ACS Nano* **2010**, *4*, 5121.
- [56] T. Uyar, P. Kingshott, F. Besenbacher, *Angew. Chem., Int. Ed.* **2008**, *47*, 9108.
- [57] D. M. Warsinger, S. Chakraborty, E. W. Tow, M. H. Plumlee, C. Bellona, S. Loutatidou, L. Karimi, A. M. Mikelonis, A. Achilli, A. Ghassemi, L. P. Padhye, S. A. Snyder, S. Curcio, C. D. Vecitis, H. A. Arafat, J. H. Lienhard, *Prog. Polym. Sci.* **2018**, *81*, 209.
- [58] N. Scharnagl, H. Buschatz, *Desalination* **2001**, *139*, 191.
- [59] Y. Yan, *Developments in Fibers for Technical Nonwovens*, Elsevier Ltd, Amsterdam, Netherlands **2016**.
- [60] B. Ledesma, S. Román, A. Álvarez-Murillo, E. Sabio, C. M. González-García, *J. Therm. Anal. Calorim.* **2014**, *115*, 537.
- [61] S. Xie, S. Wu, S. Bao, Y. Wang, Y. Zheng, D. Deng, L. Huang, L. Zhang, M. Lee, Z. Huang, *Adv. Mater.* **2018**, *30*, 1800683.
- [62] J. Liu, S. Wang, T. Huang, P. Manchanda, E. Abou-Hamad, S. P. Nunes, *Sci. Adv.* **2020**, *6*, eabb3188.
- [63] J. R. Moran, J. L. Ericson, E. Dalcanale, J. A. Bryant, C. B. Knobler, D. J. Cram, *J. Am. Chem. Soc.* **1991**, *113*, 5707.
- [64] P. Roncucci, L. Pirondini, G. Paderni, C. Massera, E. Dalcanale, V. A. Azov, F. Diederich, *Chem. Eur. J.* **2006**, *12*, 4775.
- [65] M. Torelli, I. Domenichelli, A. Pedrini, F. Guagnini, R. Pinalli, F. Terenziani, F. Artoni, R. Brighenti, E. Dalcanale, *Synlett* **2018**, *29*, 2503.
- [66] M. Torelli, F. Terenziani, A. Pedrini, F. Guagnini, I. Domenichelli, C. Massera, E. Dalcanale, *ChemistryOpen* **2020**, *9*, 261.
- [67] P. J. Skinner, A. G. Cheetham, A. Beeby, V. Gramlich, F. Diederich, *Helv. Chim. Acta* **2001**, *84*, 2146.
- [68] R. Bag, Y. Sikdar, S. Sahu, D. K. Maiti, A. Frontera, A. Bauzá, M. G. B. Drew, S. Goswami, *Dalton Trans.* **2018**, *47*, 17077.
- [69] J. V. Milić, F. Diederich, *Chem. Eur. J.* **2019**, *25*, 8440.